Sains Malaysiana 42(6)(2013): 819–826

Methylene Blue Adsorption on Graphene Oxide

(Penjerapan Metilena Biru ke Atas Grafin Oksida)

CHIN HUA CHIA*, NUR FAZLINDA RAZALI, MOHD SHAIFUL SAJAB, SARANI ZAKARIA, NAY MING HUANG & HONG NGEE LIM

ABSTRACT

In this study, graphene oxide (GO), produced using the simple Hummer's method, was used as adsorbent to remove methylene blue (MB) from aqueous solution. Characterizations using transmission electron microscope (TEM) and Fourier transform infrared (FTIR) spectroscopy were carried out on the GO before the MB adsorption experiments. The adsorption kinetics and isotherm studies were conducted under different conditions (pH = 3-7 and MB concentration = 100-400 mg/L) to examine the adsorption efficiency of the GO towards MB in aqueous solution. The adsorption kinetics data were analyzed using different kinetic models to investigate the adsorption behavior of MB on GO. The obtained results showed that the maximum adsorption capacity of the GO towards MB can achieve up to ~700 mg/g for the adsorption at 300 mg/L MB. The adsorption kinetic data were found to fit pseudo-second order model as compared with pseudo-first-order model. The intraparticle diffusion model suggested that the adsorption process of GO towards MB was dominated by the external mass transfer of MB molecules to the surface of GO.

Keywords: Adsorption isotherm; adsorption kinetics; intraparticle diffusion; methylene blue

ABSTRAK

Dalam penyelidikan ini, grafin oksida (GO) yang disediakan melalui kaedah Hummer telah digunakan sebagai bahan penjerap untuk menyingkirkan metilena biru (MB) daripada larutan akues. Pencirian menggunakan mikroskop elektron transmisi (TEM) dan spektroskopi inframerah transmisi Fourier (FTIR) telah dilakukan ke atas GO sebelum eksperimen penjerapan MB. Data kinetik penjerapan telah dianalisis dengan menggunakan model kinetik yang berlainan untuk mengkaji sifat penjerapan MB ke atas GO. Keputusan yang diperoleh menunjukkan bahawa kapasiti penjerapan maksimum GO terhadap MB mencapai ~700 mg/g daripada larutan MB berkepekatan 300 mg/L. Data kinetik penjerapan didapati berpadanan dengan model pseudo-tertib kedua. Model resapan intrazarah mencadangkan bahawa proses penjerapan MB ke atas GO adalah didominasi oleh pemindahan jisim luaran molekul MB ke permukaan GO.

Kata kunci: Isoterm penjerapan; kinetik penjerapan; metilena biru; resapan intrazarah

INTRODUCTION

Graphene, a two dimensional and one-atom thick carbon, has attracted attention in the past several years due to its excellent electronic, thermal, optical and mechanical properties (Novoselov et al. 2004). Recently, graphene and graphene oxide (GO) have been widely used in developing nanocomposites materials for different applications, such as antibacterial paper (Pasricha et al. 2009), drug carrier (Yang et al. 2009), lithium ion battery (Xue et al. 2011), photocatalyst (Zhang et al. 2011), biosensor (Shan et al. 2010; Yang et al. 2011a) and supercapacitor (Wang et al. 2010). GO is highly oxygenated and hydrophilic which can be well dispersed in water. GO has a large theoretical specific surface area (as high as 2620 m^2/g) with huge number of functional groups, i.e., hydroxyl, epoxyl and carboxyl, which can immobilize diverse organic and inorganic substances (Zhu et al. 2010).

Activated carbon is one of the most widely used adsorbent materials for wastewater treatment to remove heavy metal ions and hazardous dyes (Tan et al. 2008). Besides, carbon nanotubes have also been proven to be a promising adsorbent for hydrogen (Hou et al. 2003), heavy metal ions (Lu & Chou 2006) and dye compounds (Gong et al. 2009; Yao et al. 2010) due to their relatively large specific area. Recently, graphene and graphene oxide has started to attract attention from researchers as adsorbent in removing heavy metal ions (Deng et al. 2010) and dyes (Ramesha et al. 2011; Yang et al. 2011b) from aqueous solutions.

In the present study, GO was produced via Hummer's method and it was then being used to investigate its adsorption efficiency towards methylene blue (MB) in aqueous solutions at different parameters, including pH, MB concentration, time and temperature. The obtained adsorption experiment data were then analyzed and interpreted using different models, such as pseudo kinetic models, Langmuir and Freundlich isotherms and Van't Hoff theory, to investigate the adsorption behavior of MB on GO.

Experimental Methods

Synthesis of Graphene Oxide (GO)

GO used in this study was prepared using Hummers' method (Hummers & Offeman 1958) with slight modification. We use a simple one pot oxidation process without the tedious temperature control and mixing steps. Firstly, oxidation process was carried out by mixing H_2SO_4 (400 mL), graphite flakes (3 g) and $KMnO_4$ (18 g) using a magnetic stirrer for 3 days to allow the completion of graphite oxidation. The color of the mixture changed from dark purplish green to dark brown. H_2O_2 solution was then added into the mixture to stop the oxidation process and the color of the mixture changed to bright yellow, indicating high oxidation level of graphite oxide. The graphite oxide formed was then washed with HCl solution (1 M) for 3 times and deionized water repeatedly for 10 times until the pH of the product reached 4-5. The washing process was carried out using centrifugation technique. During the washing with deionized water, the graphite oxide experienced exfoliation, leading to thickening of the GO solution and resulted in the formation of GO gel. The obtained gel was freeze-dried to obtain solid GO.

Characterizations of GO

The morphology and shape of the produced GO were analyzed using a transmission electron microscope (TEM - Philips, CM-12) operated at 100 kV. Prior to the test, each sample was ultrasonicated for 10 min, then dropped gently onto the carbon coated copper-grid aided with micropipette and left to dry at room temperature (20°C). The Fourier transform infrared (FTIR) examination of the GO was conducted using Perkin Elmer GX spectrophotometer in the range of 4000-400 cm^{-1}.

Adsorption Kinetics Experiment of MB on GO

Adsorption experiments were carried out at different parameters, including pH and initial concentration of MB and temperature. Briefly, 0.1 g of GO was added into a flask containing 100 mL of MB solution. The initial pH was previously adjusted using 0.01 M HCl or 0.01 M NaOH. The temperature of the solution was controlled using a water bath with temperature regulator. The mixture was stirred at a constant speed 250 r.p.m. using a mechanical stirrer for 6 h. Aliquots of solution (~0.1 mL) were withdrawn at various intervals of time, centrifuged and the concentration of MB was determined using a microplate reader (Versamax). The amount of MB adsorbed at time t, q_t (mg/g), was calculated using $q_t = \frac{(C_0 - C_t)V}{m}$, where C_0 is the initial concentration of MB (mg/L) and C_t is the amount of adsorbed MB on the adsorbent (mg/g). V is the volume of the solution (mL) and m is the amount of adsorbent (g).

Adsorption Isotherm Experiment of MB on GO

Adsorption equilibrium studies were carried out by agitating a series of vials containing 0.1 g of GO and 100 mL of MB solutions with different initial concentrations (100-400 mg/L) in a thermostat rotary shaker at 20±2°C with a constant speed of 150 rpm. The procedure was repeated at temperature 40 and 60±2°C. The agitation was continued to the desired temperature for 4 h and the MB concentration of the solution samples were analyzed as described before.

Results and Discussion

Characterization of GO

Figure 1(a) shows that the electron micrograph of the produced GO sheets. The average lateral dimension of GO is around 350 nm. The IR spectrum of the GO is showed in Figure 1(b). The intense absorption peaks at 3440 and 1626 cm^{-1} correspond to the vibrations of absorbed water molecules. The absorption peaks at 1730 and 1405 cm^{-1} are due to C–O–H deformation and C=O stretching of COOH groups, respectively. The absorption bands at 1060 and 1230 cm^{-1} are due to the epoxy ring deformation and C–O stretching mixed with C–OH bending, respectively (Shen et al. 2010).

Adsorption Kinetic Experiments
Effect of Initial pH

Figure 2 shows the adsorption kinetics of GO towards MB at different pHs. The experiments were conducted at 20°C. It can be seen that the adsorption capacity of the GO increased significantly from 28.5 mg/g to 542 mg/g when the pH of the solution increased from 3 to 7. This increment can be attributed to lower competition between the MB molecules and H^+ ions in the formation of electrostatic attraction with the functional groups on the GO's surface. No adsorption was noticed at pH9 which might due probably to the hydrolysis of the GO at high pH and created positively charged sites on the GO (Batzias & Sidiras 2007). This condition resulted in electrostatic repulsion between the GO and MB molecules. Besides, the high pH condition might also change the molecular structure of the MB due to stepwise demethylation (Batzias & Sidiras 2007). Therefore the pH7 was selected for further adsorption experiments.

Effect of Initial MB Concentration

Adsorption experiments were carried out with different initial MB concentrations, ranging from 100 to 300 mg/L. Figure 3 shows the effect of initial concentration of MB on adsorption kinetics of the GO. The adsorption capacity of the GO increased with increasing initial concentration of MB. The GO can uptake up to 700 mg/g of MB for the adsorption process carried out at 300 mg/L of MB. The high concentration of adsorbate has been proven to be

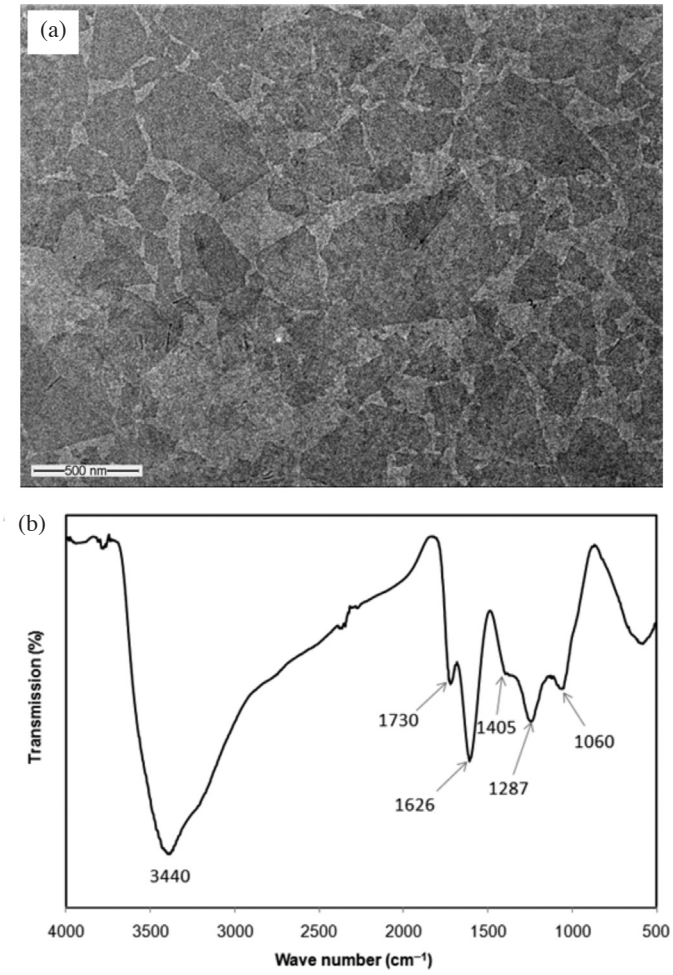

FIGURE 1. (a) TEM micrograph of GO taken at magnification 10 000× and (b) IR spectrum of the GO

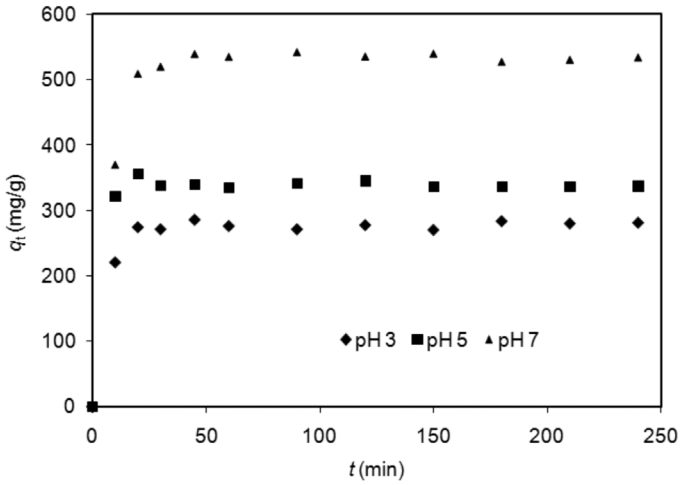

FIGURE 2. Effect of pH on adsorption kinetics of MB on GO (C_0 = 100 mg/L; Temperature = 293 K)

able to provide driving force to oppose the mass transfer resistance between the aqueous and solid phases (Sajab et al. 2011). In addition, it was also found that the higher the MB concentration, the longer the time for attainment of adsorption equilibrium. However, the adsorption equilibrium can be achieved much faster than that of previous reported results on the adsorption of MB on kenaf core fibres (Sajab et al. 2011). For the same MB

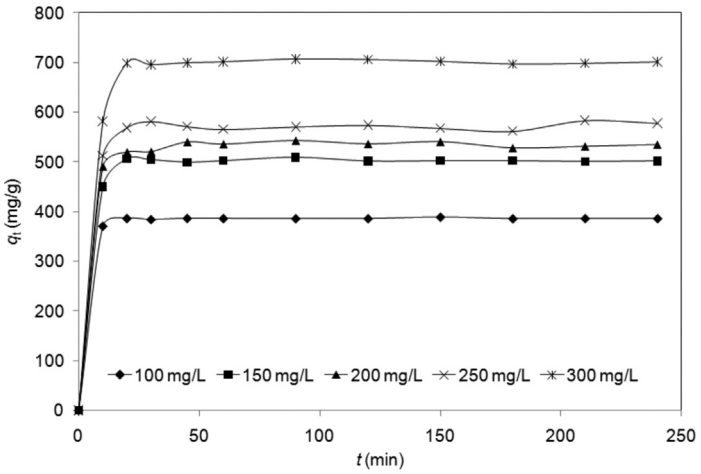

FIGURE 3. Effect of initial concentration of MB on adsorption kinetics (pH = 7; Temperature = 293 K)

concentration, i.e. 300 mg/g MB, the kenaf core fibres required about 120 min to achieve equilibrium with adsorption capacity of about 185 mg/g MB, whereas, in the present study, GO took about 25 min of equilibrium time with the adsorption capacity of around 700 mg/g. This can be attributed to the large specific area and two dimensional structure of GO, which do not require diffusion into inner porous structure of the adsorbent.

ADSORPTION KINETICS AND MECHANISM PSEUDO-FIRST AND PSEUDO-SECOND ORDER MODELS

The adsorption kinetics data obtained from the adsorption experiments were analyzed using the pseudo-first order and pseudo-second order models. The equations of the models are as follow:

Pseudo-first order (Lagergren 1898):

$$\ln (q_e - q_t) = \ln q_e - k_1 t, \quad (1)$$

where q_e and q_t are the amounts of adsorbed MB on the adsorbent (mg/g) at equilibrium and at time t, respectively, and k_1 is the pseudo-first order rate constant (min^{-1}). This model assumes that the adsorption rate of adsorbate with time is directly proportional to the difference in adsorption capacity at equilibrium and the adsorbed amount.

Pseudo-second order (Ho & McKay 1999):

$$\frac{t}{q_t} = \frac{1}{k_2 q_e^2} + \frac{1}{q_e} t, \quad (2)$$

where k_2 is the rate constant of pseudo-second order. This model assumes that the rate-limiting step involves chemisorption of adsorbate on the adsorbent. By fitting the experimental data (Figure 4(a)), the adsorption rate constant for each model was calculated and summarized in Table 1. As can be seen from the table, the kinetics data were well fitted by the pseudo-second order, as demonstrated by the higher regression coefficents (r^2) obtained. In addition, the calculated q_e values for the pseudo-second order is highly matched with the the experimental data as compared with those of the pseudo-first order model. This indicated that the adsorption kinetics of MB on GO was not diffusion controlled.

INTRAPATICLE DIFFUSION MODEL

Besides the pseudo-first and pseudo-second oder models, the kinetics data were also analyzed using the intraparticle diffusion model (Sajab et al. 2011). There are two main diffusions processes, i.e. surface mass transfer and intraparticle diffusions, which can be investigated by plotting the q_t against $t^{1/2}$ according to the equation $q_t = k_i t^{1/2} + I$, where k_i is the intraparticle diffusion constant and I is the intercept (mg/g) (Weber & Morris 1963). Figure 4(b) shows the plots of q_t versus $t^{1/2}$ of the adsorption kinetics data for different inital MB concentration. It can seen that at low MB concentrations (100 and 150 mg/L), the plots show single linear section, whereas as the MB concentration increased, the plots show two linear sections. The calculated values of the k_i and I are presented in Table 2. The value of $k_{i,1}$ is much higher than $k_{i,2}$, and it increased with increasing initial MB concentration. This revealed that the adsorption at low MB concentration may be dominated by the mass transfer process, which can due probably to the geometry of GO. As shown in the TEM result, the produced GO is in a form of thin sheet without porosity. Therefore, the MB molecules can be readily accessed and adsorbed on the surface functional groups of GO. This is unlike in the case of the adsorption using activated carbon (Dural et al. 2011; Karagöz et al. 2008) and bio-adsorbent materials (Annadurai et al. 2002; Sajab et al. 2011), which possesses high porosity and therefore the adsorption process involved both external film and intraparticles diffusions. For the adsorption at higher MB concentrations, the existance of second straight line

TABLE 1. Pseudo-first order and pseudo-second order kinetics model parameters for adsorption of MB on GO at 293 K

Initial MB concentration (mg/L)	$q_{e\,exp}$ (mg/g)	Pseudo-first order			Pseudo-second order		
		$q_{e\,cal}$ (mg/g)	k_1 (min^{-1})	r^2	$q_{e\,cal}$ (mg/g)	k_2 (g/mg min)	r^2
100	385.76	13.29	0.01	0.252	384.6	0.0002	1
150	501.78	19. 65	0.007	0.140	500.0	0.0002	1
200	534.22	49.55	0.012	0.305	526.3	0.0021	1
250	578.16	34.50	0.008	0.159	588.2	0.0017	0.999
300	701.02	34.81	0.012	0.271	714.3	0.0004	0.999

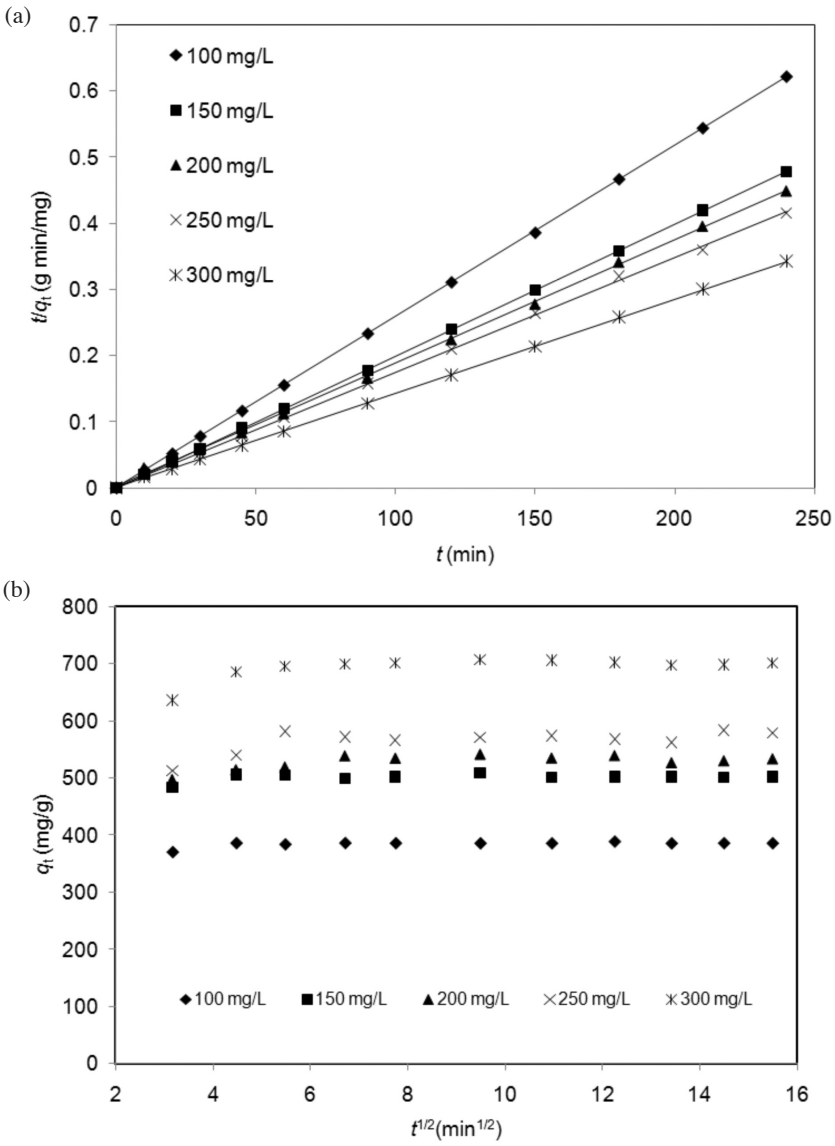

FIGURE 4. Adsorption kinetics models of MB on GO: (a) pseudo-second order and (b) intraparticle diffusion

may be due to the rearrangement of the MB molecules which were initially adsorbed on the GO, as schematically demonstrated in Figure 5. This process may require longer time to achieve the adsorption equilibrium.

ADSORPTION ISOTHERM OF MB ON GO

In this study, Langmuir and Freundlich isotherms were applied to the batch adsorption experimental data. The Langmuir isotherm model assumes monolayer coverage of the adsorbate over a homogenous adsorbent surface,

TABLE 2. Intraparticle diffusion model parameters for adsorption of MB on GO at 293 K

Initial MB concentration (mg/L)	First straight line			Second straight line		
	$k_{i,1}$ (mg/g min$^{1/2}$)	I_1 (mg/g)	r^2	$k_{i,2}$ (mg/g min$^{1/2}$)	I_2 (mg/g)	r^2
100	6.151	353.2	0.705	0.009	386.0	0.998
150	9.154	458.0	0.758	0.061	503.0	0.999
200	9.676	468.7	0.948	0.089	545.7	0.997
250	20.92	446.4	0.999	0.092	561.7	0.998
300	26.84	559.6	0.773	0.121	705.1	0.998

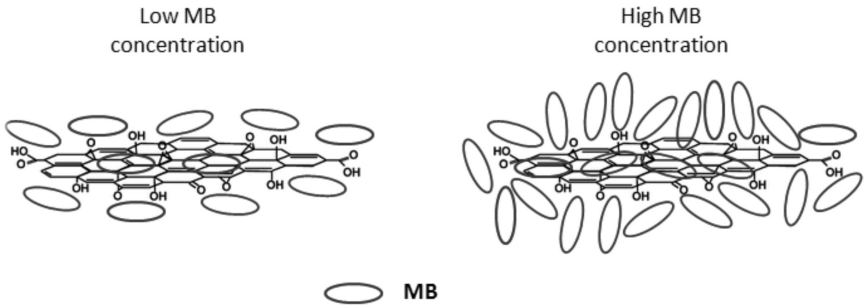

FIGURE 5. Schematic of adsorption of MB on GO at low and high MB concentration

with each molecule adsorbed onto the surface having the same adsorption activation energy. The Langmuir isotherm is expressed as:

$$\frac{C_e}{q_e} = \frac{1}{Q_{0b}} + \frac{C_e}{Q_0}, \tag{3}$$

where Q_0 is the maximum adsorption capacity per unit mass of adsorbent (mg/g) and b is a constant related to the adsorption energy (L/mg).

The Freundlich isotherm describes reversible adsorption onto heterogeneous surfaces and is not restricted to the formation of the monolayer of adsorbate. The Freundlich isotherm is expressed as:

$$\ln q_e = \ln K_F + \frac{1}{n} \ln C_e, \tag{4}$$

where K_F and $1/n$ are the Freundlich constants, with K_F represents the relative adsorption capacity of the adsorbent and n represents the degree of dependence of adsorption on the equilibrium concentration of MB.

The Langmuir and Freundlich constants were calculated from the slopes and intercepts of the plots of C_e/q_e versus C_e and ln q_e versus ln C_e (graph not shown), and the obtained results are summarized in Table 3. The data for the adsorption of MB on the GO were well fitted by the Langmuir isotherm model, as demonstrated by the high correlation coefficients (r^2) obtained compared to those for the Freundlich isotherm model. This has further confirmed the monolayer adsorption of MB onto the GO. As can be seen that the value of Q_0 and K_F increased with the increase of temperature, indicating that the adsorption is favorable at high temperatures.

A similar trend has also been observed from the study of removing MB using carbon nanotubes (Yao et al. 2010). This could be attributed to the increase of mobility of the MB molecules and the decrease of viscosity of the solution at elevated temperature. However, an opposite trend with activated carbon (Dural et al. 2011) was observed which might be due to the different adsorption mechanisms for the adsorption of MB on the activated carbon. A dimensionless constant, R_L was also calculated using equation $R_L = \frac{1}{1+bC_m}$, where C_m is the highest initial MB concentration (mg/L).

TABLE 3. Calculated equilibrium constants for adsorption of MB on GO at different temperatures

Temperature (°C)	Langmuir isotherm				Freundlich isotherm		
	Q_0 (mg/g)	b (mg/L)	r^2	R_L	K_F	n	r^2
20	476.2	0.189	0.999	0.017	246.1	8.183	0.948
40	484.2	0.215	0.999	0.015	256.8	8.217	0.925
60	493.7	0.230	0.999	0.014	288.5	10.000	0.981

The value of R_L obtained for the adsorption at three different temperatures is higher than zero and less than unity, revealing the favorable of the adsorption of MB on GO (Sajab et al. 2011).

THERMODYNAMIC PARAMETERS

The thermodynamic parameters ($\Delta G°$, $\Delta H°$ and $\Delta S°$) of the adsorption of MB on GO were calculated using equations $K_D = \frac{\Delta S°}{R} - \frac{\Delta H°}{RT}$ and $\Delta G° = -RT \ln K_D$, where R is the ideal gas constant, T is the temperature (K) and K_D is the distribution coefficient calculated from the experiment. The values of $\Delta H°$ and $\Delta S°$ were calculated from the slope and intercept of the Van't Hoff plots (Figure 6) and listed in Table 4. The positive value of $\Delta H°$ suggested that the adsorption process is endothermic. The negative value of $\Delta G°$ indicates that the adsorption is spontaneous. The positive value of $\Delta S°$ confirmed the increased randomness at solid/solution interface during the adsorption process.

Based on the high adsorption rate and capacity, the GO produced in this study was found to be a suitable alternative adsorbent of the commercial activated carbon for the removal of cationic dyes from non acidic wastewater effluents. The adsorption data was found to follow the pseudo-second order kinetic model with regression coefficient (r^2) higher than 0.99, suggesting the chemisorption behavior of MB on GO. The intraparticle diffusion model suggested that the adsorption process was dominated by the external mass transfer of MB molecules to the surface of GO.

CONCLUSION

Graphene oxide (GO) has been produced via simple Hummer's method. The methylene blue (MB) adsorption studies showed that the produced GO exhibits maximum adsorption capacity 700 mg/g, which is relatively higher than that of other adsorbent materials. The isotherm adsorption data well fitted the Langmuir model, suggesting the monolayer adsorption of MB onto the GO. The intraparticle diffusion model suggested that the adsorption process of GO towards MB was dominated by the external mass transfer of MB molecules to the surface of GO.

ACKNOWLEDGEMENTS

The authors acknowledge the financial support given by Universiti Kebangsaan Malaysia via the research project grants UKM-GGPM-NBT-085-2010, UKM- UKM-FST-07-FRGS0233-2010 and OUP-FST-2012.

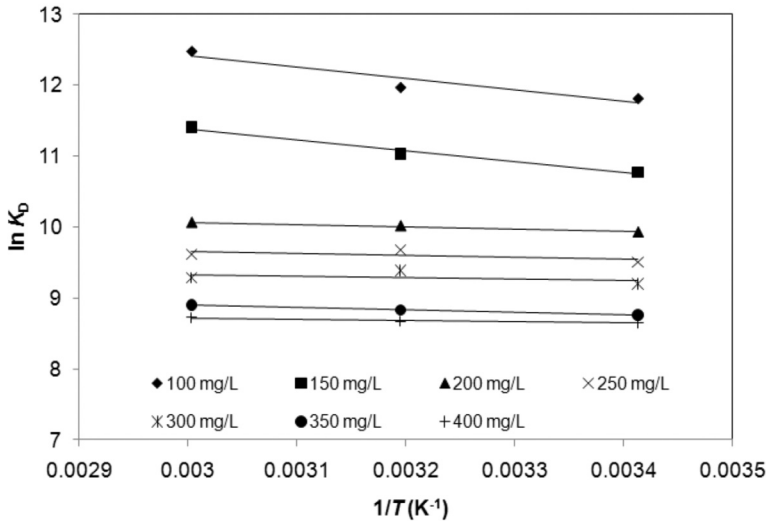

FIGURE 6. Plots of ln K_D versus $1/T$ for adsorption of MB on GO

TABLE 4. Thermodynamic parameters for the adsorption of MB onto GO

Concentration of MB (mg/L)	$\Delta H°$ (kJ/mol)	$\Delta S°$ (J/mol K)	$\Delta G°$ (kJ/mol)		
			293 K	313 K	333 K
100	13.32	143.1	–28.62	–31.48	–34.35
150	12.64	132.5	–26.18	–28.83	–31.48
200	2.750	91.91	–24.18	–28.68	–30.61
250	2.451	87.61	–23.22	–27.34	–29.17
300	1.755	82.81	–22.51	–25.84	–27.58
350	2.844	82.52	–21.33	–25.75	–27.48
400	1.528	77.04	–21.04	–24.04	–25.66

REFERENCES

Annadurai, G., Juang, R-S. & Lee, D-J. 2002. Use of cellulose-based wastes for adsorption of dyes from aqueous solutions. *Journal of Hazardous Materials* B92: 263-274.

Batzias, F.A. & Sidiras, D.K. 2007. Simulation of dye adsorption by beech sawdust as affected by pH. *Journal of Hazardous Materials* 141: 668-679.

Deng, X., Lu, L., Li, H. & Luo, F. 2010. The adsorption properties of Pb(II) and Cd(II) on functionalized graphene prepared by electrolysis method. *Journal of Hazardous Materials* 183: 923-930.

Dural, M.U., Cavas, L., Papageorgiou, S.K. & Katsaros, F.K. 2011. Methylene blue adsorption on activated carbon prepared from *Posidonia oceanica* (L.) dead leaves: Kinetics and equilibrium studies. *Chemical Engineering Journal* 168: 77-85.

Gong, J-L., Wang, B., Zeng, G-M., Yang, C-P., Niu, C-G., Niu, Q-Y., Zhou, W-J. & Liang, Y. 2009. Removal of cationic dyes from aqueous solution using magnetic multi-wall carbon nanotube nanocomposite as adsorbent. *Journal of Hazardous Materials* 164: 1517-1522.

Ho, Y.S. & McKay, G. 1999. Pseudo-second order model for sorption processes. *Process Biochemistry* 34: 451-465.

Hou, P-X., Xu, S-T., Ying, Z., Yang, Q-H., Liu, C. & Cheng, H-M. 2003. Hydrogen adsorption/desorption behavior of multi-walled carbon nanotubes with different diameters. *Carbon* 41: 2471-2476.

Hummers, W.S. & Offeman, R.E. 1958. Preparation of graphitic oxide. *Journal of American Chemical Society* 80: 1339-1339.

Karagöz, S., Tay, T., Ucar, S. & Erdem, M. 2008. Activated carbons from waste biomass by sulfuric acid activation and their use on methylene blue adsorption. *Bioresource Technology* 99: 6214-6222.

Lagergren, S. 1898. About the theory of so-called adsorption of soluble substance. *Kungliga Svenska. Vetenskapsakademiens. Handlingar*: 21: 1-39.

Lu, C. & Chou, H. 2006. Adsorption of zinc(II) from water with purified carbon nanotubes. *Chemical Engineering Science* 61: 1138-1145.

Novoselov, K.S., Geim, A.K., Morozov, S.V., Jiang, D., Zhang, Y., Dubonos, S.V., Grigorieva, I.V. & Firsov, A.A. 2004. Electric field effect in atomically thin carbon films. *Science* 306: 666-669.

Pasricha, R., Gupta, S. & Srivastava, A.K. 2009. A facile and novel synthesis of Ag-graphene-based nanocomposites. *Small* 5: 2253-2259.

Ramesha, G.K., Vijayakumar, A., Muralidhara, H.B. & Sampath, S. 2011. Graphene and graphene oxide as effective adsorbents towards anionic and cationic dyes. *Journal of Colloid and Interface Science* 361: 270-277.

Sajab, M.S., Chia, C.H., Zakaria, S., Jani, S.M., Ayob, M.K., Chee, K.L., Khiew, P.S. & Chiu, W.S. 2011. Citric acid modified kenaf core fibres for removal of methylene blue from aqueous solution. *Bioresource Technology* 102: 7237-7243.

Shan, C., Yang, H., Han, D., Zhang, Q., Ivaska, A. & Niu, L. 2010. Graphene/AuNPs/chitosan nanocomposites film for glucose biosensing *Biosensors and Bioelectronics* 25: 1070-1074.

Shen, X., Wu, J. & Zhou, H. 2010. One-pot solvothermal synthesis and magnetic properties of graphene-based magnetic nanocomposites. *Journal of Alloys and Compounds* 506: 136-140.

Tan, I.A.W., Ahmad, A.L. & Hameed, B.H. 2008. Adsorption of basic dye on high-surface-area activated carbon prepared from coconut husk: Equilibrium, kinetic and thermodynamic studies. *Journal of Hazardous Materials* 154: 337-346.

Wang, B., Park, J., Wang, C., Ahn, H. & Wang, G. 2010. Mn_3O_4 nanoparticles embedded into graphene nanosheets: Preparation, characterization, and electrochemical properties for supercapacitors. *Electrochimica Acta* 55: 6812-6817.

Weber, W.J. & Morris, J.C. 1963. Kinetics of adsorption on carbon from solution. *Journal of Sanitary Engineering Division* 89: 31-59.

Xue, X-Y., Ma, C-H., Cui, C-X. & Xing, L-L. 2011. High lithium storage performance of α-Fe_2O_3/graphene nanocomposites as lithium-ion battery. *Solid State Sciences* 13: 1526-1530.

Yang, M., Javadi, A. & Gong, S. 2011a. Sensitive electrochemical immunosensor for the detection of cancer biomarker using quantum dot functionalized graphene sheets as labels. *Sensors and Actuators B: Chemical* 155: 357-360.

Yang, S-T., Chen, S., Chang, Y., Cao, A., Liu, Y. & Wang, H. 2011b. Removal of methylene blue from aqueous solution by graphene oxide. *Journal of Colloid and Interface Science* 359: 24-29.

Yang, X., Zhang, X., Ma, Y., Huang, Y., Wang, Y. & Chen, Y. 2009. Superparamagnetic graphene oxide-Fe_3O_4 nanoparticles hybrid for controlled targeted drug carriers. *Journal of Materials Chemistry* 19: 2710-2714.

Yao, Y., Xu, F., Chen, M., Xu, Z. & Zhu, Z. 2010. Adsorption behavior of methylene blue on carbon nanotubes. *Bioresource Technology* 101: 3040-3046.

Zhang, Z., Sun, Y., Cui, X. & Jiang, Z. 2011. A green and facile synthesis of TiO_2/graphene nanocomposites and their photocatalytic activity for hydrogen evolution. *International Journal of Hydrogen Energy* 37: 811-815.

Zhu, Y.W., Murali, S., Cai, W.W., Li, X.S., Suk, J.W., Potts, J.R. & Ruoff, R.S. 2010. Graphene and graphene oxide: Synthesis, properties, and applications. *Advanced Materials* 22: 3906-3924.

Chin Hua Chia*, Nur Fazlinda Razali, Mohd Shaiful Sajab, Sarani Zakaria
School of Applied Physics, Faculty of Science and Technology
Universiti Kebangsaan Malaysia
43600 Bangi, Selangor
Malaysia

Nay Ming Huang
Low Dimensional Materials Research Centre
Physics Department, University of Malaya
50603 Kuala Lumpur
Malaysia

Hong Ngee Lim
Department of Chemistry
Faculty of Science, Universiti Putra Malaysia
43400 UPM Serdang, Selangor
Malaysia

*Corresponding author; email: chia@ukm.my

Received: 13 June 2012
Accepted: 13 September 2012